A MULTIDIMENSIONAL OPTIMIZATION APPROACH TO IMPROVE MODULE EFFICIENCY, POWER AND COSTS

Jibran Shahid, Max Mittag, Martin Heinrich
Fraunhofer Institute for Solar Energy Systems ISE, Heidenhofstraße 2, 79110 Freiburg, Germany
jibran.shahid@ise.fraunhofer.de

ABSTRACT: In the design of common solar modules, one of the main tasks is to achieve maximum output power or efficiency. Due to the complex interaction between different parameters of PV materials and module configuration this is a difficult task. The complexity increases when costs attributed to components and processes have to be considered. We use an approach to optimize module power and costs simultaneously based on the cell-to-module ratio which is usually used to describe the impact of module design and materials on module power. We present optimization routines to identify ideal module configurations. We apply five different types of optimization algorithms to the cell-to-module model, to find the optimal values of input parameters that maximize module power and efficiency and minimize the respective cell-to-module losses as well as the specific module costs [€/Wp]. The algorithms applied within this study are evaluated regarding their accuracy towards optimal output of the PV module and their computing power. We optimize a 285 W reference module and increase power by 5.8% and efficiency by 0.45 $\%_{abs}$. Specific costs are reduced by 0.9 €ct/Wp.

Keywords: Cell-to-module ratio, CTM, Multidimensional optimization, efficiency, power, costs

1. INTRODUCTION

Integrating solar cells into a PV module causes different loss and gain mechanisms leading to a module power that is different from the power of the solar cells before module integration [1–4]. The cell-to-module efficiency ratio $CTM_{efficiency}$ describes the ratio between the module efficiency and the mean efficiency of the solar cells before integration (Figure 1).

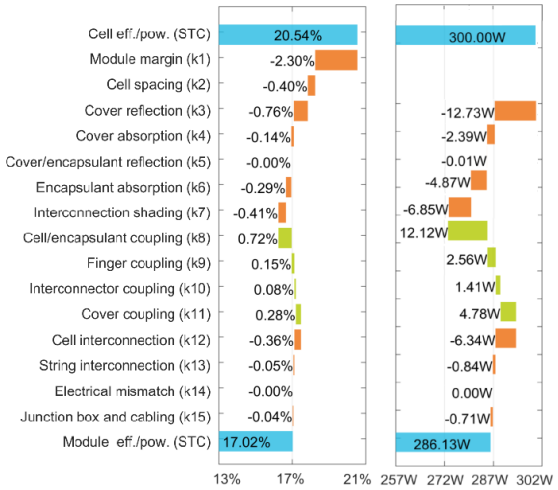

Figure 1: Cell-to-module (CTM) loss and gain factors for an exemplary photovoltaic module.

Module design and materials are chosen to achieve high CTM ratios to maximize the electrical power output or efficiency. In order to reduce the losses and increase the gains related to module integration, a profound understanding of all factors that influence the module output is essential.

Hädrich *et. al.* proposed a methodology to calculate CTM ratios and to analyze PV modules regarding efficiency and power changes resulting from the integration of solar cells into modules [5]. The methodology presented by Hädrich *et. al.* is based on 13 different factors to describe gains and losses attributed to module components, physical effects or important interfaces. In previous work, we added two electrical k-factors, extended the model for additional module concepts and performed detailed analyses of single components and loss factors [6–8].

In this paper, we present an approach based on a combination of CTM analysis, cost modelling and optimization algorithms. We apply different optimization algorithms in order to minimize CTM losses and specific costs [€/Wp] simultaneously. We evaluate optimization algorithms on the basis of their accuracy towards optimal output of the PV module and their computing power.

2. APPROACH

Our work is based on the CTM methodology as proposed by Hädrich *et. al.* and several extensions as presented earlier [2, 6, 8–11]. In this work we describe the optimization using algorithms and a cost model that has been added to the existing set of models.

2.1. Objective function of the system

In order to apply the optimization algorithms, an objective function has to be implemented for the output of the CTM model that defines the targeted value. In this objective function, decision variables and constant variables should be recognized.

$$PV\ output = f(x_1, x_2, \dots, x_n, y_1, y_2, \dots, y_n) \quad (1)$$

In (1) f is a function that describes the optimization target: the CTM ratio, the output of the PV module or the specific cost of the PV module. Decision variables x_n can be changed within the optimization and y_n are constant variables that are fixed within the optimization. Simply speaking, the decisions variables are those input parameters a module manufacturer can influence and modify such as cell distance, ribbon cross section etc. while the constant variables are not directly accessible for optimization.

The user can either define one parameter as a decision variable or a number of parameters for optimization. All other variables will act as a constant y_n for the objective function.

Once the objective function has been implemented, different algorithms can be applied and the results of the

optimization algorithms can be compared on the basis of criteria given above. Several optimization algorithms are applied to this CTM model in order to optimize either the output power or efficiency or cost of the PV module. Additionally, optimization algorithms can be applied simultaneously in order to increase efficiency or power and at the same time reducing the cost of the module.

2.2. Optimization algorithms

Five different optimization algorithms are used in this study. The algorithms are chosen on the basis of their different optimization approach and popularity.

The first algorithm is the Nelder-Mead Algorithm (NMA) which is most commonly used in a numerical method which does not require the derivative of the objective function [12]. The second algorithm is the Interior Point algorithm (IPM) which is widely used to solve linear and nonlinear optimization problems [13]. The last three algorithms come in the category of random search method; names are Particle Swarm Optimization (PSO), Crow Search Algorithm (CSA) and Antlion Optimization (ALO) [14–16]. These algorithms are based on a random search method and use search agents in order to converge to the solution. The number of search agents used in this study is 20 for each random search algorithm.

The comparing criteria among these algorithms are computing power and the time taken to converge to the optimum result. If the algorithm is able to reach the optimum result, the computing power is measured and the number of iterations is counted. The last factor is related to convergence time which also depends on the performance of the machine on which the algorithm is running.

2.3. Selected optimization parameters

We demonstrate the optimization using selected parameters as decision variables. The parameters selected for this study are cell and string distance, the width and thickness of the cell ribbon and the thickness of the front glass. Constraints for these parameters are set as shown in Table I.

Table I: Boundaries of selected parameters.

[mm]	Min	Ref.	Max
Cell distance	0.5	2	10
String distance	0.5	2	10
Cell ribbon width	0.5	1.5	2.5
Cell ribbon thickness	0.05	0.2	0.3
Front glass thickness	1	3.2	10

In the given range, some of the values are not practically applicable. For example, 1 mm front glass thickness is not a common thickness. In reality a glass with this thickness is more expensive compared to common thicknesses of 2 to 4 mm. In order to use 1 mm front glass, also other measures have to be taken into account, e.g. the frame type. We extended parameter boundaries i.e. of glass and cell ribbon thickness to check the capabilities of the algorithms. For practical application parameter limits can be adjusted easily.

Cell and string distance play an important role in increasing the efficiency, power and specific cost of the PV module. In order to understand the effects of variations of these parameters on the output of the PV module, we perform a detailed analysis.

When the cell gap increases (and the module size is adapted accordingly), the inactive area share becomes larger, which increases the loss factor attributed to cell spacing (k2, see [5]). Cell spacing losses belong to the geometrical effects which describe the efficiency, but not the power of the PV module. An increase in inactive area reduces module efficiency (Figure 2).

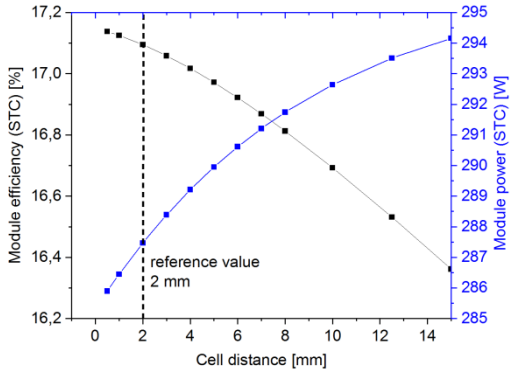

Figure 2: Efficiency and power graph for cell distance.

An increase in module power due to internal reflection gains is attributed to a separate factor k11 [7]. An increase in cell distance increases the electrical losses in ribbons (k12) due to the additional ribbon lengths. The change in string distance affects the losses in string ribbons (k13) accordingly. Gains from k11 show a non-linear, flattening behavior with the increase of cell distance while k2 and k12 (electrical losses in ribbons) increase linearly with cell distance. Therefore an optimum cell spacing exists.

Width and thickness for interconnector ribbons are parameters that can be influenced by a module manufacturer in order to avoid losses. Increasing the thickness of the cell interconnector will not increase the shading of the active cell area but lower the resistance. Due to this the output power and efficiency increases with the cell ribbon's thickness (Figure 3).

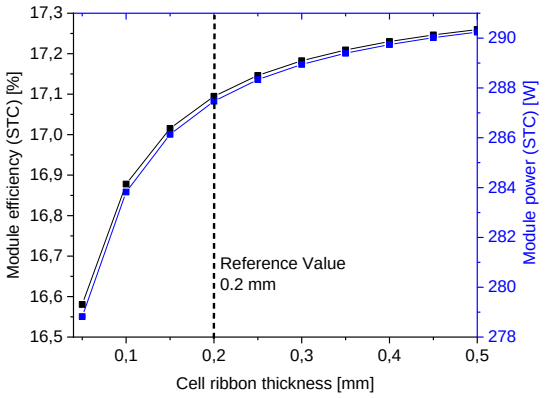

Figure 3: Efficiency and power graph for cell ribbon thickness.

The width of the ribbon affects the shading of active cell area (k7). Assuming a cell with continuous busbars, shading will occur if the width of the ribbon exceeds the busbar width. With the ribbon width, the cross section of the ribbon changes, affecting the resistive losses (k12). Therefore, the cross section area of cell ribbon should be increased without active area shading. Additionally, gains from reflection from the ribbon to the solar cell occur

(k10). Depending on cell metallization, ribbon properties and the electrical currents an optimum regarding power and efficiency for interconnector dimensions exists. The optimum width might not be the width of the busbar (Figure 4).

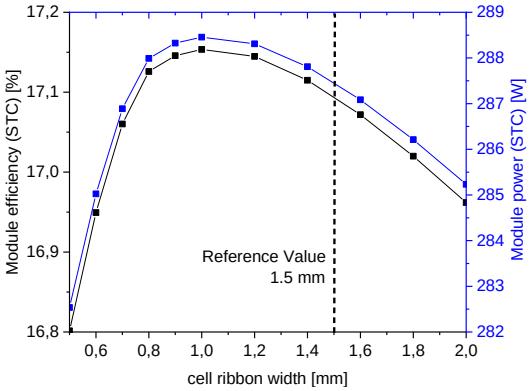

Figure 4: Power and efficiency for a variation of the ribbon width. The continuous busbars on the cell have a width of 0.8 mm.

2.4. Cost modelling

To perform an optimization of specific costs (€/Wp) we create a cost model that considers material costs of relevant components as well as manufacturing costs. Manufacturing costs include equipment (4.5%), facility (1.0%), labor (6.0%), spare parts (1.0%), utilities (5.0%) and waste disposal costs (0%). We use a combined surcharge of 17.5% of the material costs as manufacturing overhead (which are approx. 15% of the total reference module costs as displayed in Figure 5) based on data extracted from the SCost model [17].

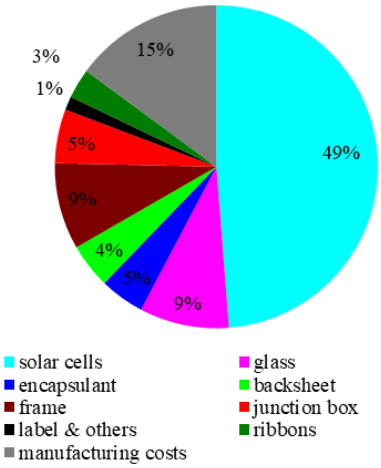

Figure 5: Cost structure of a reference module

We use the module specifications (size etc.) and the module material costs to calculate the costs shares of different module areas as shown in Figure 6. We distinguish costs related to inactive areas (i.e. cell spacing), cost related to active areas (solar cell), cost that are independent of module dimensions (i.e. junction boxes and labels) and costs depending on the circumference (frame). As can be seen in Figure 6, active area (with cells) displays the highest costs within the module due to the large area share. Calculating the cost per area, the inactive and active area cost the same (not considering cells).

Inactive area contributes to a certain extent to module power generation (backsheet gains) [8]. Inactive area power gains increase with larger cell spacing but additional gains become marginal when increasing cell distances. Costs increase linearly with module size. Therefore an optimum exists regarding the size of the inactive areas and the attributed power.

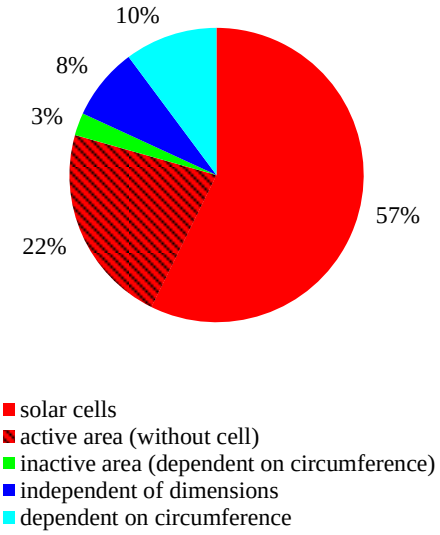

Figure 6: Area cost share structure of a reference module

Specific module costs (€/Wp) use the total module costs as described above and the module power. Since module power results from the combination of initial cell power and CTM effects, module integration and CTM power changes need to have an impact on specific costs.

We calculate the power losses attributed to different CTM factors and combine those results with the cost model. Our results are discussed below.

2.5. Reference module

In order to evaluate the results of the optimization algorithms, a reference study is performed. We assume a module consisting of 60 H-pattern solar cells with 5 continuous busbars (156x156 mm², I_{MPP} = 8.571 A). The initial cell efficiency is 20.54% (5.00 Wp). Additional parameters of commercially available module materials (encapsulant etc.) are used as input. Reference values of the selected materials are given in Table I.

We perform a CTM analysis of the reference module and find the output power to be 286.1 W_p which corresponds to a CTM_{power} ratio of 0.95. The module efficiency is 17.02 % with a $CTM_{efficiency}$ ratio of 0.83. This result from the reference study will be used to compare the results of the optimization algorithms. The cost of ownership for the reference module setup are calculated 72.95 € which gives the specific cost 25.5 €ct/W_p.

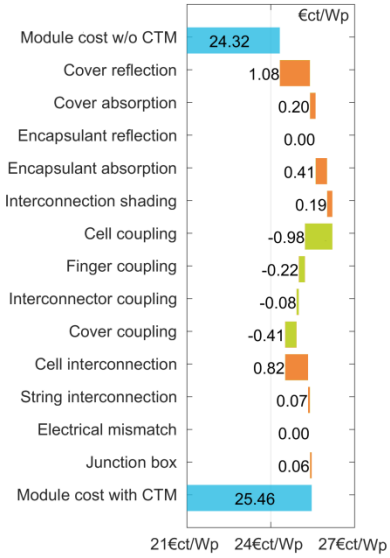

Figure 7: Waterfall diagram of specific cost of the module with and without CTM power changes.

3. CASE STUDIES

A few of the available module configuration parameters are selected as decision variables. The selected parameters for this study are the cell and the string distance, the width and thickness of the cell ribbon and the thickness of the front glass. Other input parameters remain constant. We apply the algorithms and perform a module optimization regarding power, efficiency and specific costs. All calculations are performed assuming standard testing conditions (STC).

3.1. Power of the PV module

The first optimization is related to the output power of the PV module. As displayed in Figure 8 the different algorithms find a different optimum. A maximum module power of 302.9 W_p is calculated. The NMA, PSO and IPM are able to reach the highest possible output power. They set the cell and string distance to their upper boundary which is 10 mm. By increasing the cell gap, the backsheet reflection gain can be increased.

Algorithms also reduce the width of the cell connector to 0.9 mm in order to reduce the ribbon shading losses. Since a reduction in ribbon width increases the electrical losses of the cell connector, the algorithms increase the thickness of the cell connector in order to compensate and to reduce the resistive losses.

The glass thickness is also reduced to 1 mm to its lower boundary from its initial value of 3.2 mm in the reference module.

The efficiency of the module is 16.61%, which is less than our reference study. This is due to fact that the cell spacing and the total module area increased. Therefore the inactive area share increased lowering the efficiency. The power maximization also reduces the specific cost of this module to 24.7 €ct/W_p.

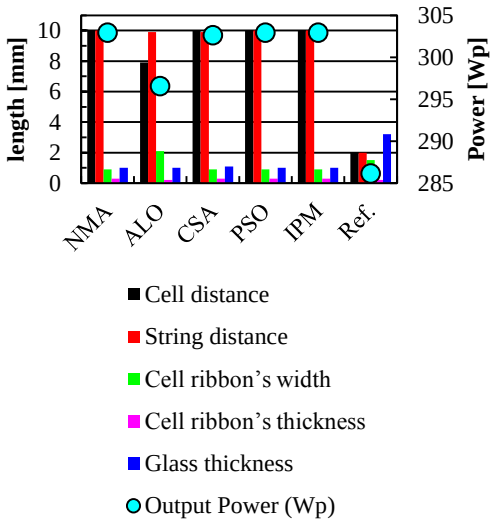

Figure 8: Module power and selected input parameters after application of optimization algorithms on CTM modelling.

Among the algorithms with accurate results, the fastest is achieved by IPM, which only takes 9 iterations and reaches the maximum power in only 4.75 seconds as shown in Table II. All random search algorithms are unable to reach the optimum result. Nonetheless, CSA, a random search algorithm, is ranked second. It takes 20 iterations and approximately 13 seconds to reach the second highest power which is 302.62 W_p. In comparison to the other algorithms, the weakest result is achieved by ALO which takes around 14.8 seconds and 20 iterations and achieved 296.55 W_p .

Table II: Algorithms results in terms of their computing power, time and accuracy.

	Objective f(x) evaluations count	Algorithm Iteration	Search agents	Time Lapse (sec)	Deviation from optimal value ($_{abs}$)
NMA	242	147	-	17.0	0.0
ALO	500	20	20	14.8	-6.35
CSA	201	20	20	15.5	-0.28
PSO	200	20	20	15.3	0.0
IPM	66	10	-	7.2	0.0

3.2. Efficiency of the PV module

The second study focusses on the efficiency of the PV module. As we mention before, efficiency is affected by changes in inactive module area. Therefore efficiency optimization includes power, active and inactive module areas.

The highest module efficiency calculated is 17.47%, which is 0.45%$_{abs.}$ more than the reference study. In this study, again the NMA, CSA and IPM are able to reach the highest efficiency. The algorithms reduce the cell and string distance to their lower boundary, which is 0.5 mm

as shown in Figure 9. The width of the cell ribbon also decreases to 0.9 mm, algorithms predict this result due to fact that it will decrease the shading of the cell and also this width will not lead to severe electrical losses. The small cell gap reduces cell spacing losses. Beside this, cell ribbon losses also decrease. The IPM, CSA and NMA have identical results. The thickness of the cell connector is 0.3 mm and the top glass thickness is 1 mm which are same that we have observed in Section 3.1.

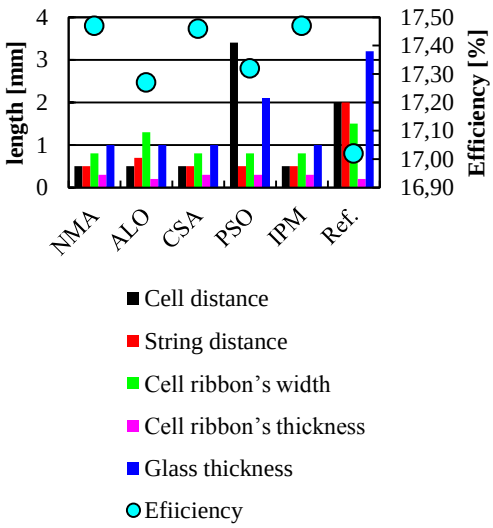

Figure 9: Module efficiency and selected input parameters after application of optimization algorithms on CTM-modelling.

The area of the PV module is reduced because of the reduced cell and string distance, this also results in the lower cost of ownership value which is 74.4 €, but in comparison to the previous study, the specific cost increas to 25.73 €ct/W_p. This is because the output power is reduced to 289.21 W_p by achieving the highest efficiency.

Table III: Algorithms results in terms of their computing power, time and accuracy.

	Objective f(x) evaluations count	Algorithm Iteration	Search agents	Time Lapse (sec)	Deviation from optimal value ($_{abs}$)
NMA	285	172	-	18.9	0.0
ALO	500	20	20	15.3	-0.2
CSA	201	20	20	17.7	-0.01
PSO	60	6	20	4.7	-0.15
IPM	133	20	-	8.89	0.0

As shown in Table III, once again the IPM achieves the highest efficiency within the given constraints. The IPM takes 20 iterations in 8.89 seconds, whereas the NMA takes 172 iterations in 18.09 seconds to reach the same result as IPM. The second promising result is calculated by the PSO, which calculates 2.1 mm optimal glass thickness. Beside this, the cell distance is 3.4 mm and 0.50 mm string distance. The NMA and IPM predict 0.8 mm to be the optimal width of the cell connector to reach the highest efficiency. In this study, the least optimum result is observed by ALO, which calculates an optimum efficiency of 17.27%. PSO takes around 20 iterations in 14.80 seconds, which is the longest time among all algorithms.

3.3. Specific Cost of the PV module

In the third study, the specific costs of the PV module are optimized which are defined as the cost per watt peak at STC. Calculations now have to include models for module power, active and inactive area and their respective costs.

The same set of input parameters as in the other studies is used. We assume that the costs of materials (i.e. the front glass) remain constant even if material parameters change (i.e. the thickness). Therefore, we only consider changes in module area (absolute and relative) and ribbon lengths to be cost relevant. We are also assuming that the cross-sectional area of the cell ribbon does not influence cost.

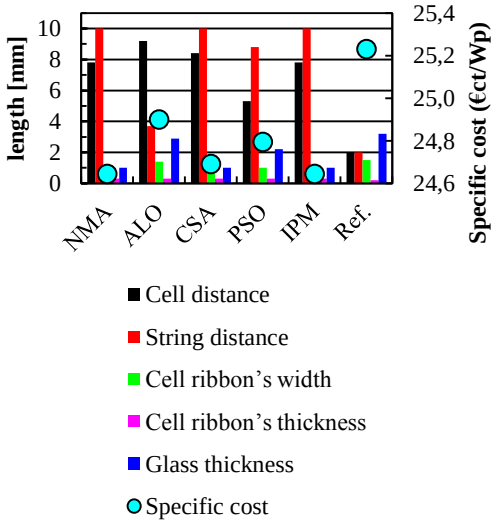

Figure 10: Specific module costs and selected input parameters after application of optimization algorithms on cost and CTM-modelling.

After performing all calculations using the different optimization algorithms we find the results displayed in Figure 10. The cell and string distance are set to their upper boundaries which is 10 mm. The width and thickness of the cell connector are 0.9 mm and 0.3 mm and the thickness of the glass is 1 mm which is the same as we have observed in our last two studies related to power and efficiency. The NMA and IPM find the lowest specific cost of the module with 24.6 €ct/W_p. This specific cost is only 0.1 €ct/W_p less than what we have observed in the first study related to optimization of power of the PV module.

CSA reaches the second minimum specific cost within 15 seconds and takes 20 iterations as shown in Table IV. Among the best three algorithms which reach the least specific cost, IPM is the fastest to achieve the optimum result in 8.5 seconds and NMA is slowest (23.9 seconds, 154 iterations) to reach the same result. The algorithm calculating the highest costs in this study is ALO, which calculates 24.9 €ct/ W_p in 15.3 seconds.

Table IV: Algorithms results in terms of their computing power, time and accuracy.

	Objective f(x) evaluations count	Algorithm Iteration	Search agents	Time Lapse (sec)	Deviation from optimal value ($_{abs}$)
NMA	252	154	-	23.9	0.0
ALO	500	20	20	15.3	-0.26
CSA	201	20	20	15.0	-0.05
PSO	60	6	20	4.2	-0.15
IPM	121	19	-	8.5	0.0

3.4. Extended constraints

Among all studies, IPM and NMA performed well regarding the quality of the result and computation time. All the random search algorithms are unpredictable in terms of their results, they have to run several time in order to reach the same result which was obtained by IPM and NMA in a single run. Out of three random search algorithms only CSA performed well in the Section 3.3 and PSO performed well in Section 3.1 but not in others studies. Other than that, NMA was able to reach the same result as IPM, but it takes more computational power and time. Due to this, we carried all the above studies using IPM and extended constraints of the selected parameters. So far in order to increase the output power and reduce the specific cost, all the algorithms selected the upper boundary of cell and string distance. On the other hand, algorithms selected the lower boundaries of cell and string distance in order to increase the efficiency.

In this study, we have extended the constraints of cell distance, string distance and the thickness of the cell connector beyond practical values as shown in Table V to analyze additional effects.

Table V: Constraints of the selected input parameters

[mm]	Min	Ref.	Max
Cell distance	0.5	2	100
String distance	0.5	2	100
Cell connector width	0.05	0.2	0.35

We perform three optimization runs (module power, module efficiency and specific costs). Results are displayed in Table VI.

Optimizing for maximum power now leads to 310.2 Wp. We observe a significant increase in cell and string distance. The algorithm predicted an optimal cell distance of 31.4 mm and string distance should be 49.8 mm. Differences between string and cell spacing result from the specific resistance of string and cell ribbons. Beside this the width of the cell connector is also increased to 1 mm in order to handle the current increase in the PV module. The remaining parameters (cell ribbon thickness and front glass thickness) reach the same values as we have observed in previous studies.

Optimizing the module efficiency, IPM suggests the same set of values that was predicted in the Section 3.2 except for the width of the cell connector. Here the width of cell connector decreases to 0.8 mm. As the cell gap (and therefore the backsheet gain) is reduced in this study, the reduced cross-sectional area of the cell connector is sufficient to limit the electrical losses in the module. The efficiency achieved in this study is 17.52% which is 0.05 $\%_{abs}$ higher than what we observe in Section 3.2.

Table VI: Result of the revised first three studies using different boundaries.

	Power	Efficiency	Specific Costs
Cell distance (mm)	31.50	0.50	7.90
String distance (mm)	49.80	0.50	11.40
Cell ribbon width (mm)	1.00	0.80	0.90
Cell ribbon thickness (mm)	0.30	0.30	0.30
Glass thickness (mm)	1.00	1.00	1.00
Module power (Wp)	310.6	290.0	303.4
Efiiciency (%)	12.87	17.52	16.71
Specific cost (€ct/Wp)	26.2	25.0	24.6
Objective f(x) evaluations count	128	60	197
Algorithm Iteration	18	9	29
Time Lapse (sec)	10.24	4.01	13.00

While optimizing the specific cost of the module, the algorithm tries to reduce it. This means that output power will also be increased simultaneous while reducing the cost of ownership. In this study, we observe a change in cell distance to 7.9 mm and a string distance of 11.4 mm. The specific cost achieved in this study is 24.6 €ct/W_p and the output power of the module is 303.4 W_p. Previously in Section 3.3, we have observed that the algorithms have predicted the same set of parameters which was observed in Section 3.1, but in this study, the algorithm has predicted a significantly different result than the study related to the output power of the module.

Regarding the optimization we find the choice of boundaries to be relevant. No "automatic" module optimization appears to be possible without deriving constraints from manufacturing (i.e. technical limits for glass sizes or thicknesses) or final module use. The additional consideration of PV systems and power plants is required for module optimization at this point. An unrestricted use of module parameters as derived from optimization will not be possible without creating conflicts in module use. Especially, the importance of mounting and installation as well as the share of system costs may be mentioned here [18].

CONCLUSION & SUMMARY

We add a cost model and different algorithms for module optimization to existing cell-to-module (CTM) analysis models. The prior enables us to perform an analysis regarding specific module costs (€/Wp) for flexible module layouts. The latter allows the multi-dimensional optimization of modules.

We apply these extensions and optimize a reference module regarding module power, efficiency and specific costs by selecting five input parameters for optimization.

Results of the multidimensional power optimization show an increase in module power of 16.8 Wp (+5.9%) compared to the reference module and assuming the same initial cell power. The CTM_{power} increased from 0.95 to 1.01. An increase in module efficiency by $0.45\%_{abs}$ is observed after optimizing the efficiency of the reference module. As the specific cost of the reference module is 25.5 €ct/W_p, with the optimization 24.6 €ct/W_p is reached.

We observe that increasing the cell and string distance will increase the output power of the module, but show that there is a limit on increasing the cell gap beyond practically relevant boundaries for spacing. Other than this, the algorithms optimize the cross-sectional area of the cell ribbon according to the output power. We observe that the higher power module requires a larger cross-sectional area due to increase in maximum power point. The cross-sectional area is decreased, when the output power of module decreases.

In this study, we have assumed that front glass thickness and the cell ribbon cross-section do not influence cost . In future, we would like to add cost dependencies with input parameters of the PV module integration and try to make the optimization model more robust.

We used the algorithms NMA, ALO, CSA, PSO and IPM in this study. In this paper we have carried out 3 studies using all algorithms. In each study, the random search algorithms i.e. ALO, CSA and PSO delivered varying results. Random search algorithms have to run several time on the optimization problem in order to reach the optimum. Sometimes they got stuck in local minima were not able to reach the global minima. So far only PSO was able to reach the optimum in the study related to output power optimization and CSA was able to reach the optimum in specific cost. Besides this, the most promising algorithm is IPM for this application. NMA is also able to achieve the same result that was obtained by IPM, but it takes more computing power and time. Beside them, all the random search algorithms were not able to achieve the desired results.

ACKNOWLEDGEMENT

We would like to thank the German Ministry of Economic Affairs and Energy (FKZ 0324033) for their funding.

REFERENCES

[1] ITRPV, “International Technology Roadmap for Photovoltaic (ITRPV): Results 2017, Ninth Edition,” 2018.

[2] M. Mittag *et al.*, “Systematic PV module optimization with the cell-to-module (CTM) analysis software,” *Photovoltaics International*, no. 36, pp. 97–104, 2017.

[3] I. Hädrich *et al.*, “PV Module efficiency analysis and optimization,” PV-Rollout, Boston, Massachusetts, USA, 2011.

[4] H. Wirth *et al.*, *Photovoltaic Modules: Technology and Reliability*. Berlin/Boston: De Gruyter, 2016.

[5] I. Hädrich *et al.*, “Unified methodology for determining CTM ratios: Systematic prediction of module power,” *Solar Energy Materials and Solar Cells*, vol. 131, pp. 14–23, 2014.

[6] M. Mittag *et al.*, “Electrical and thermal modeling of junction boxes,” 33rd EUPVSEC, Amsterdam, 2017, pp. 1501–1506.

[7] M. Mittag *et al.*, “Analysis of backsheet and rear cover reflection gains for bifacial solar cells,” *33rd European PV Solar Energy Conference and Exhibition*, vol. 2017.

[8] M. Mittag *et al.*, “Cell-to-Module (CTM) analysis for photovoltaic modules with shingled solar cells,” in *44th IEEE PV Specialist Conference PVSC*.

[9] N. G. Dhere, “Comparison of optical transmittance spectra of new tempered glass with that of superstrate glass extracted from a field-aged PV module,” Sandia National Laboratories Photovoltaics Program Tech Brief #: 26 MDRC-10/10/99, 1999.

[10] N. Woehrle *et al.*, “Solar cell demand for bifacial and singulated-cell module architectures,” *36th Photovoltaics International*, pp. 48–62, 2017.

[11] C. Reise *et al.*, “From bifacial PV cells to bifacial PV power plants: The chain of characterization and performance prediction,” *Photovoltaics International*, no. 38, pp. 1–10, 2018.

[12] J. C. Lagarias *et al.*, “Convergence Properties of the Nelder--Mead Simplex Method in Low Dimensions,” *SIAM J. Optim.*, vol. 9, no. 1, pp. 112–147, 1998.

[13] J. Gondzio, “Interior point methods 25 years later,” *European Journal of Operational Research*, vol. 218, no. 3, pp. 587–601, 2012.

[14] S. Mirjalili, “The Ant Lion Optimizer,” *Advances in Engineering Software*, vol. 83, pp. 80–98, 2015.

[15] F. Marini *et al.*, “Particle swarm optimization (PSO). A tutorial,” *Chemometrics and Intelligent Laboratory Systems*, vol. 149, pp. 153–165, 2015.

[16] A. Askarzadeh, “A novel metaheuristic method for solving constrained engineering optimization problems: Crow search algorithm,” *Computers & Structures*, vol. 169, pp. 1–12, 2016.

[17] S. Nold *et al.*, “Cost modeling of silicon solar cell production innovation along the PV value chain,” in *27th EUPVSEC 2012, Frankfurt, Germany, 2012*.

[18] Ran Fu, David Feldman, Robert Margolis, Mike Woodhouse, and Kristen Ardani, “U.S. Solar Photovoltaic System Cost Benchmark: Q1 2017,”